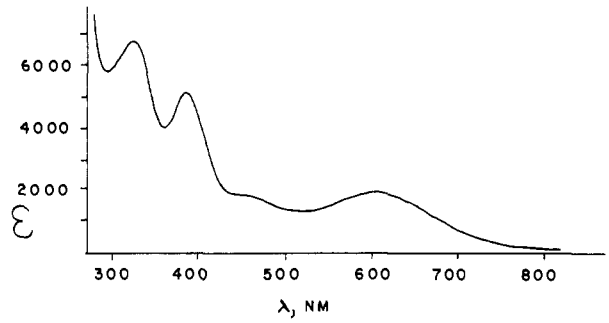

Figure 4. Electronic absorption spectra of **1** in glassed glycerol/DMF (3:1) at 80 K.

LMCT, the near-UV absorptions and the LF absorption (a measure of the shift in the Cu(II) HOMO) of **1** all shift in the same direction relative to the monomer. Other workers have reported that σ(thiolate) → Co(III) LMCT is not significantly shifted by the additional ligation of thiolate to either Ag(I) or CH_3Hg^+.[23] However, adduct formation resulted in the relatively small decreases in the average ligand field of the $Co^{III}N_5S$ and $Co^{III}N_4OS$ chromophores. Monomer spectra in DMF at 80 K do not contain a high-energy absorption corresponding to the intense band at ≈327 nm for **1**. This additional absorption in **1** therefore, is presumably associated with the Cu(I) sites. An absorption at ≈365 nm has been attributed to the Cu(I)–thiolate sites of a mixed-valence, mixed-metal Cu(I)–Co(III) tetramer and assigned as Cu(I) → S(thiolate) MLCT.[24] We wish to refrain from analyzing the spectra of **1** further until the electronic structure of the monomer becomes established. Toward this end, a combination of molecular orbital[25] and detailed spectroscopic studies of the monomer are being pursued.

Acknowledgment. Research at Rutgers was supported in part by the NSF (Grant CHE-8417548) and the David and Johanna Busch Foundation. The X-ray diffraction/crystallographic computing facility at Rutgers was purchased with NIH Grant 1510 RRO 1486 01A1. Research at the University of Illinois was supported by the National Institutes of Health (Grant HL13652).

Supplementary Material Available: Tables of anisotropic thermal parameters, hydrogen atom parameters, bond distances and angles for the $[(SCH_2CH(CO_2CH_3)NHCH_2-)_2]$ ligands and perchlorate groups, and calculated and experimental magnetic susceptibility data (5 pages); a table of observed and calculated structure factors (16 pages). Ordering information is given on any current masthead page.

(23) Heeg, M. J.; Elder, R. C.; Deutsch, E. *Inorg. Chem.* **1979**, *18*, 2036.

(24) Lane, R. H.; Pantaleo, N. S.; Farr, J. K.; Coney, W. M.; Newton, M. G. *J. Am. Chem. Soc.* **1978**, *100*, 1610 and references cited therein.

(25) Westbrook, J.; Krogh-Jespersen, K., unpublished results.

Contribution from the Department of Chemistry, Purdue University, West Lafayette, Indiana 47907

Multiply Bonded Octahalodiosmate(III) Anions. 3.[1] Synthesis and Characterization of the Octahalodiosmate(III) Anions $[Os_2X_8]^{2-}$ (X = Cl, Br). Crystal Structure Determinations of Two Forms of $(PPN)_2Os_2Cl_8$ (PPN = Bis(triphenylphosphine)nitrogen(1+))

Phillip E. Fanwick, Stephen M. Tetrick, and Richard A. Walton*

Received August 19, 1986

The triply bonded octahalodiosmate(III) anions $[Os_2X_8]^{2-}$ (X = Cl, Br) are formed by the reactions of the diosmium(III) carboxylates $Os_2(O_2CR)_4Cl_2$ (R = CH_3, n-C_3H_7) with gaseous HX in ethanol and have been isolated as their n-Bu_4N, Ph_4As, and PPN (bis(triphenylphosphine)nitrogen(1+)) salts. These complexes are essentially diamagnetic, they behave as 1:2 electrolytes in acetonitrile, and they have IR and electronic absorption spectra that accord with this formulation. Their electrochemical properties (cyclic voltammetry in 0.1 M TBAH–CH_2Cl_2) reveal the existence of an accessible one-electron oxidation ($E_{p,a} \simeq +1.1$ V vs. Ag/AgCl) and an irreversible one-electron reduction at $E_{p,c} \simeq -0.9$ V vs. Ag/AgCl. These anions are believed to have the $\sigma^2\pi^4\delta^2\delta^{*2}$ ground-state electronic configuration; since there is no net δ component to the Os–Os bonding, free rotation of the OsX_4 units about the Os–Os bond can occur. In accord with this expectation, two crystalline forms of $(PPN)_2Os_2Cl_8$ have been isolated from CH_2Cl_2–diethyl ether solutions, one green (**1**) and the other brown (**2**), in which different rotational geometries are encountered. The crystal data for **1** at −190 °C are as follows: space group $P2_1/c$; a = 23.167 (4) Å; b = 13.423 (4) Å; c = 22.867 (5) Å; β = 107.80 (3)°; V = 6771 (6) Å^3; Z = 4. For **2**, the crystal data at 22 °C are as follows: space group $C2/c$; a = 33.415 (6) Å; b = 13.692 (2) Å; c = 21.634 (4) Å; V = 6798 (5) Å^3; Z = 4. In both structures a disorder is present that is of a type encountered in other $[M_2X_8]^{n-}$ species, in which the Os–Os unit is randomly present in two orientations with the major orientation having an occupancy of ca. 70% for both **1** and **2**. The Os–Os distance is very short in **1** and **2**, viz., 2.206 (1) and 2.212 (1) Å for the major orientation, respectively. In **1** the disorder is such that there are two different staggered rotational geometries for the major and minor orientations (χ = 11.4 [8] and 39.8 [14]°, respectively), while for **2** the $[Os_2Cl_8]^{2-}$ units are rigorously eclipsed. These results indicate that, for the $[Os_2Cl_8]^{2-}$ anion, crystal-packing forces rather than nonbonded Cl···Cl repulsions dictate the rotational geometry.

Introduction

In the development of multiple metal–metal bond chemistry, the notion of isoelectronic relationships between dimetal cores has helped in the expansion of this field to different metals. For example, such reasoning led to persistent, and eventually successful, attempts to isolate complexes of the quadruply bonded $(W\equiv W)^{4+}$ core that were isoelectronic with those of Re_2^{6+} and Mo_2^{4+}.[2,3] Among the important classes of such complexes are homoleptic halide anions of the type $[M_2X_8]^{n-}$ (X = F, Cl, Br, I). These species have been found to possess metal–metal bond orders of

(1) Part 2: Agaskar, P. A.; Cotton, F. A.; Dunbar, K. R.; Falvello, L. R.; Tetrick, S. M.; Walton, R. A. *J. Am. Chem. Soc.* **1986**, *108*, 4850.

(2) (a) Cotton, F. A.; Walton, R. A. *Multiple Bonds between Metal Atoms*; Wiley: New York, 1982. (b) Cotton, F. A.; Walton, R. A. *Struct. Bonding (Berlin)* **1985**, *62*, 1.

(3) Sattelberger, A. P.; McLaughlin, K. W.; Huffman, J. C. *J. Am. Chem. Soc.* **1981**, *103*, 2880.

0020-1669/86/1325-4546$01.50/0

3.5 or 4 and have been encountered previously only for the cases where M = Mo, W, Tc, and Re.[2,4] Very recently, we were able to extend this chemistry to include the platinum metals through our isolation of salts of the octahalodiosmate(III) anions $[Os_2X_8]^{2-}$ (X = Cl, Br). This was described in a preliminary report along with the structure of the salt $(PPN)_2Os_2Cl_8$ (PPN = bis(triphenylphosphine)nitrogen(1+)).[5] Subsequently, we undertook detailed structural studies on the salts $(n\text{-}Bu_4N)_2Os_2X_8$ (X = Cl, Br) and an appraisal of the electronic structure of the $[Os_2Cl_8]^{2-}$ anion using the SCF-Xα-SW method.[1] We now provide full details of the synthesis of salts of the $[Os_2X_8]^{2-}$ anions, their spectroscopic and electrochemical properties, and the crystallographic characterization of two forms of $(PPN)_2Os_2Cl_8$ which reveal an unexpected and novel result, namely, the existence of several rotational geometries in the solid state for the *same* salt.

Experimental Section

The diosmium(III) carboxylates $Os_2(O_2CR)_4Cl_2$ (R = CH_3 *n*-C_3H_7) were prepared as described in the literature.[6] Reagents were purchased from commercial sources and used without subsequent purification. Solvents were reagent grade and were deoxygenated prior to use. All reactions were carried out under an atmosphere of dinitrogen unless otherwise noted.

A. Reactions of $Os_2(O_2CR)_4Cl_2$ (R = CH_3, *n*-C_3H_7) with Hydrogen Halides. (i) $(PPN)_2Os_2Cl_8$. A sample of $Os_2(O_2C\text{-}n\text{-}C_3H_7)_4Cl_2$ (0.153 g, 0.191 mmol) was suspended in 10 mL of ethanol. This mixture was cooled to 0 °C with use of an ice bath, and HCl gas was passed through it for 5 min with stirring. Within 10 min the green suspension had dissolved to give a dark green solution that contained the $[Os_2Cl_8]^{2-}$ anion. A solution of (PPN)Cl (0.5 g) in ethanol (5 mL) was then added via a syringe. This caused the immediate precipitation of $(PPN)_2Os_2Cl_8$ as a pale green powder. This solid was collected by filtration and washed with ethanol and diethyl ether. Recrystallization of the crude product was performed as follows: the solid was dissolved in dichloromethane and filtered to yield a dark green solution. Ethanol was added slowly with stirring until the product began to precipitate as green crystalline plates. Precipitation was complete within a few minutes, and the solid was collected by filtration, washed with ethanol and diethyl ether, and finally dried in vacuo for 30 min; yield 0.325 g (98%). Anal. Calcd for $C_{72}H_{60}Cl_8N_2Os_2P_4$: C, 49.67; H, 3.47; Cl, 16.29. Found: C, 48.98; H, 3.43; Cl, 16.14.

An alternative procedure utilized the analogous acetate complex. A sample of $Os_2(O_2CCH_3)_4Cl_2$ (0.95 g, 1.38 mmol) was treated with a HCl-saturated ethanol solution (50 mL). This suspension was stirred and refluxed for 1.5 h to give a dark green solution, which was cooled to room temperature and then treated with an ethanol solution (20 mL) of (PPN)Cl (3.5 g). The mixture was stirred until precipitation of green $(PPN)_2Os_2Cl_8$ was complete. This product was removed by filtration, washed with ethanol several times, and purified as described above; yield 2.18 g (91%). The samples of $(PPN)_2Os_2Cl_8$ prepared in this manner have the same spectral and electrochemical properties as those prepared with use of the *n*-butyrate complex.

(ii) $(Ph_4As)_2Os_2Cl_8 \cdot 1.5CH_2Cl_2$. A dark green solution containing the $[Os_2Cl_8]^{2-}$ anion was generated from $Os_2(O_2C\text{-}n\text{-}C_3H_7)_4Cl_2$ as described in part A(i). This was treated with a solution of $(Ph_4As)Cl$ (0.25 g) in ethanol (5 mL). The product $(Ph_4As)_2Os_2Cl_8$ was precipitated by the slow addition of diethyl ether (25 mL) with stirring. The pale violet solid was removed by filtration, washed several times with ethanol followed by diethyl ether, and then dried. Recrystallization was accomplished by redissolving the sample in dichloromethane, filtering, and adding diethyl ether to the filtrate. The pale pink microcrystalline solid was collected by filtration, washed several times with ethanol and diethyl ether, and vacuum dried for 30 min; yield 66%. Anal. Calcd for $C_{49.5}H_{43}As_2Cl_{11}Os_2$: C, 38.16; H, 2.78. Found: C, 38.06; H, 2.73. The presence and amount of dichloromethane was determined by ^1H NMR spectroscopy.

(iii) $(n\text{-}Bu_4N)_2Os_2Cl_8$. A sample of $Os_2(O_2CCH_3)_4Cl_2$ (0.51 g, 0.742 mmol) was suspended in ethanol (25 mL) that had been previously saturated with HCl gas. This suspension was stirred at reflux for 1.5 h to give a dark green solution. An ethanolic solution (5 mL) of $(n\text{-}Bu_4N)Br$ (1.0 g) was then added with stirring, and the resulting solution was evaporated to low volume with use of a nitrogen stream. The dark green crystals of $(n\text{-}Bu_4N)_2Os_2Cl_8$ that precipitated were removed by filtration and washed with ethanol several times. Recrystallization was effected by dissolving the crude product in dichloromethane and filtering the solution. An equal portion of ethanol was then added to the filtrate with stirring followed by the slow addition of diethyl ether to induce precipitation of green $(n\text{-}Bu_4N)_2Os_2Cl_8$. The product was removed by filtration, washed several times with ethanol and diethyl ether, and dried in vacuo; yield 0.72 g (85%). Anal. Calcd for $C_{32}H_{72}Cl_8N_2Os_2$: C, 33.45; H, 6.32. Found: C, 32.35; H, 6.28.

(iv) $(n\text{-}Bu_4N)_2Os_2Br_8$. A sample of $Os_2(O_2C\text{-}n\text{-}C_3H_7)_4Cl_2$ (0.112 g, 0.140 mmol) was suspended in cold ethanol (10 mL). Gaseous HBr was bubbled through the stirred, chilled solution for 10 min, after which time the ice bath was removed. After 1 h, a clear dark green solution that contained the $[Os_2Br_8]^{2-}$ anion had formed. This was treated with $(n\text{-}Bu_4N)Br$ (0.85 g) in ethanol (5 mL) via a syringe. The product $(n\text{-}Bu_4N)_2Os_2Br_8$ precipitated as green microcrystals. These were removed by filtration, washed with ethanol and diethyl ether, and vacuum dried for 1 h; yield 0.179 g (85%). Anal. Calcd for $C_{32}H_{72}Br_8N_2Os_2$: C, 25.54; H, 4.82. Found: C, 25.75; H, 4.84.

This complex could be prepared in an identical manner with use of $Os_2(O_2CCH_3)_4Cl_2$ as the starting material; yield 88%.

B. Preparation of $(PPN)_2Os_2Cl_8$ Single Crystals. (i) Green Form 1. A 3-in. test tube (10 mm i.d.) was filled halfway with a concentrated dichloromethane solution of $(PPN)_2Os_2Cl_8$. This test tube was placed inside a larger diameter tube, which was then filled with diethyl ether up to a level that was a little higher than the dichloromethane level of the inner tube. The larger tube was stoppered and supported on a ring stand. Over the course of 1 week, diethyl ether slowly diffused into the dichloromethane solution to give dark green crystals of $(PPN)_2Os_2Cl_8$ that were suitable for X-ray crystallographic studies. These crystals were removed by filtration, carefully washed with ethanol and diethyl ether, and then dried.

(ii) Brown Form 2. A dilute dichloromethane solution (5 mL)of $(PPN)_2Os_2Cl_8$ was placed in a 25-mL Erlenmeyer flask. Diethyl ether (5 mL) was carefully layered on top of this solution, and the flask was set aside. After 2 weeks, crystals of the brown form of $(PPN)_2Os_2Cl_8$ that had deposited were collected and washed and dried in a manner similar to that used for the green crystalline form of $(PPN)_2Os_2Cl_8$.

C. X-ray Crystallography. General Procedures. Data were collected for both compounds on an Enraf-Nonius CAD-4 diffractometer using Mo Kα radiation (λ_α = 0.71073 Å) with a graphite crystal monochromator in the incident beam. The takeoff angle of the X-tube was 4.80°. The standard CAD-4 centering, indexing, and data collection programs were used.

Twenty-five reflections for $20° < 2\theta < 30°$ were located by a random search procedures and subsequently centered. These reflections were used to obtain the cell constants given in Table I along with other crystal data.

The scan width for each reflections was determined as $A + 0.35 \tan\theta$, where A = 0.80 for **1** and A = 0.75 for **2**. The rate for the final scan was calcualted from the preliminary scan results so that the ratio $I/\sigma(I)$ would be at least 50 and the maximum scan time would not exceed 60 s. All reflections were measured by the θ–2θ scan method. The width of the adjustable horizontal aperture at the detector was given by (1.5 + tan θ) mm with a vertical aperture of 4 mm. There standard reflections were monitored after every 1 h of beam exposure during data collection and displayed no systematic variation in intensity. All calculations were performed on a PDP 11/34 computer using the Enraf-Nonius Structure Determination Package. Corrections for anomalous dispersion were applied to all anisotropically refined atoms. The least-squares program minimized the function $w(|F_o| - |F_c|)^2$, where the weighting factor $w = 1/\sigma^2(F_o)$.

Structure solutions and refinements were carried out with use of standard methods. Hydrogen atoms were not included in the final least-squares refinement. Tables II and III list the atomic positional parameters and their errors for **1** and **2**. Tables IV and V list the intramolecular bond distances and angles associated with the $[Os_2Cl_8]^{2-}$ anions in crystals of **1** and **2**. Tables listing thermal parameters (Tables S1 and S2) and complete listings of bond distances (Tables S3 and S4) and bond angles (Tables S5 and S6) are available as supplementary material.

(i) Green Form 1. The multiplicities of the osmium atoms in this disordered structure were constrained as follows: Os(1) = Os(2) (major orientation) and Os(3) = Os(4) = 100% − Os(1) (minor orientation). Chlorine atoms Cl(11), Cl(13), Cl(21), and Cl(23) are common to both orientations and, hence, have multiplicities of 100%. The multiplicities of the chlorine atoms of the major orientation (Cl(12), Cl(14), Cl(22), Cl(24)) were set equal to the multiplicity of Os(1). The chlorine atoms about Os(3) of the minor orientation (Cl(31), Cl(32), Cl(33), Cl(34))

(4) Schrock, R. R.; Sturgeoff, L. G.; Sharp, P. R. *Inorg. Chem.* **1983**, *22*, 2801.
(5) Fanwick, P. E.; King, M. K.; Tetrick, S. M.; Walton, R. A. *J. Am. Chem. Soc.* **1985**, *107*, 5009.
(6) Behling, T.; Wilkinson, G.; Stephenson, T. A.; Tocher, D. A.; Walkinshaw, M. D. *J. Chem. Soc., Dalton Trans.* **1983**, 2109.

Table I. Crystallographic Data and Data Collection Parameters for the Green (**1**) and Brown (**2**) Forms of $(PPN)_2Os_2Cl_8$[a]

	1	**2**
formula	$Os_2Cl_8P_4N_2C_{72}H_{60}$	$Os_2Cl_8P_4N_2C_{72}H_{60}$
fw	1741.21	1741.21
space group	$P2_1/c$	$C2/c$[b]
a, Å	23.167 (4)	33.415 (6)
b, Å	13.423 (4)	13.692 (2)
c, Å	22.867 (5)	21.634 (4)
β, deg	107.80 (3)	136.62 (1)
V, Å^3	6771 (6)	6798 (5)
Z	4	4
d_{calcd}, g cm^{-3}	1.708	1.701
λ(Mo Kα), Å	0.71073	0.71073
monochromator	graphite	graphite
cryst dimens, mm	0.51 × 0.48 × 0.18	0.40 × 0.28 × 0.23
temp, °C	−190.0	22.0
μ(Mo Kα), cm^{-1}	42.10	41.93
abs cor applied	empirical[c]	empirical[d]
scan method	θ–2θ	θ–2θ
h,k,l limits	$\pm h,-k,l$	$h,k,\pm l$
2θ range, deg	4.00–45.00	4.00–45.00
F_{000}	3416.0	3416.0
unique data	9278	4816
data with $I > 3.0\sigma(I)$	6349	3774
no. of variables	486	227
largest shift/esd, final cycle	0.31	0.42
R[e]	0.067	0.044
R_w[f]	0.091	0.070
goodness of fit[g]	2.118	1.735

[a] Numbers in parentheses following certain data are estimated standard deviations occuring in the least significant digit. [b] The equivalent, nonstandard $I2/a$ cell has parameters of a = 23.103 Å, b = 13.692 Å, c = 21.634 Å, and β = 96.59°. [c] Walker, N.; Stuart, D. *Acta Crystallogr., Sect. A: Found. Crystallogr.* **1983**, *A39*, 158. [d] Flack, H. D. *Acta Crystallogr., Sect. A: Cryst. Phys., Diffr., Theor. Gen. Crystallogr.* **1977**, *A33*, 890. [e] $R = \sum||F_o| - |F_c||/\sum|F_o|$. [f] $R_w = [\sum w(|F_o| - |F_c|)^2/\sum w|F_o|^2]^{1/2}$; $w = 1/\sigma^2(F_o)$. [g] Goodness of fit = $[\sum w(|F_o| - |F_c|)^2/(N_{observns} - N_{parameters})]^{1/2}$.

had multiplicities equal to 100% − Os(1). In all least-squares refinement cycles, the multiplicity factor of Os(1) was treated as a variable subject to the constraints mentioned above.

(ii) Brown Form 2. This structure was also disordered. All chlorine atoms were common to both orientations and have multipliticities of 100%. The osmium atoms were constrained and refined in a manner identical with that described above for the osmium atoms in the green form **1** (see part C(i)).

Further details of the data set and the structure solution and refinement may be obtained from Dr. P. E. Fanwick of this department.

D. Physical Measurements. Electronic absorption spectra were recorded on dichloromethane solutions with an IBM 9420 spectrophotometer. Far-infrared spectra of Nujol mulls on polyethylene disks were performed on an IBM IR/98 spectrometer. Evans magnetic susceptibility measurements[7] of dichloromethane solutions of the complexes were measured on a Varian XL-200 NMR spectrometer at which the proton resonance frequency was 200 MHz. Cyclic voltammetry experiments were performed as described previously[8] on dichloromethane or acetonitrile solutions containing 0.1 M tetra-*n*-butylammonium hexafluorophosphate (TBAH) as supporting electrolyte and were referenced to the Ag/AgCl electrode at room temperature and are uncorrected for junction potentials. Samples of the green (**1**) and brown (**2**) forms of $(PPN)_2Os_2Cl_8$ were heated in argon-filled capillaries using a Melt-Temp heating device. Elemental microanalyses were performed by Dr. H. D. Lee of the Purdue University microanalytical laboratory.

Results and Discussion

The reactions between anhydrous ethanol solutions saturated with HX gas (X = Cl, Br) and the known diosmium(III) carboxylates $Os_2(O_2CR)_4Cl_2$ (R = CH_3, n-C_3H_7)[6] generate dark green solutions of the octahalodiosmate(III) anions $[Os_2X_8]^{2-}$. Suspensions of the *n*-butyrate complex react within minutes to produce solutions of the anions at 0 °C, while reflux conditions are necessary when the corresponding acetate complex is used as the starting material. This difference in reaction conditions probably reflects the insolubility of $Os_2(O_2CCH_3)_4Cl_2$, while $Os_2(O_2C$-n-$C_3H_7)_4Cl_2$ is slightly soluble in this solvent. Extended reflux times should be avoided since under these conditions the octahalodiosmate(III) anions decompose to produce the well-known hexahaloosmate(IV) anions $[OsX_6]^{2-}$. The use of anhydrous conditions is necessary because when these reactions were performed previously with use of concentrated aqueous hydrohalic acids, cleavage of the osmium–osmium triple bond in $Os_2(O_2C$-$CH_3)_4Cl_2$ occurred to produce the hexahaloosmate(IV) anions.[6]

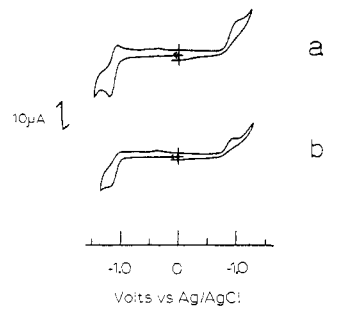

Figure 1. Cyclic voltammograms (measured in 0.1 M TBAH–CH_2Cl_2 at a Pt-bead electrode): (a) $(n$-$Bu_4N)_2Os_2Cl_8$; (b) $(n$-$Bu_4N)_2Os_2Br_8$. The sweep rate used was 200 mV/s.

The addition of ethanol solutions containing very large cations to solutions of $[Os_2X_8]^{2-}$ yields green (X = Cl, Br; cation = PPN^+, n-Bu_4N^+) or brown-pink (X = Cl; cation = Ph_4As^+) crystalline products in excellent yields.[9] All of these salts can be handled in the air with no apparent decomposition both in the solid state and in solution.

Samples of $(PPN)_2Os_2Cl_8$ and $(n$-$Bu_4N)_2Os_2Cl_8$ dissolved in acetonitrile to give solutions that had conductivities (Λ_m = 225 and 250 Ω^{-1} cm^2 mol^{-1} for $c_m = 1 \times 10^{-3}$ and 0.62×10^{-3} M, respectively) typical of those expected for 2:1 electrolytes in this solvent.[10] Solutions of the $[Os_2Cl_8]^{2-}$ salts in 0.1 M tetra-*n*-butylammonium hexafluorophosphate (TBAH)–CH_2Cl_2 have cyclic voltammograms that display a couple corresponding to a one-electron oxidation of the anion at $E_{1/2} \simeq +1.15$ V vs. Ag/AgCl (Table VI and Figure 1). This process is not chemically reversible as judged by controlled-potential electrolysis experiments. A second process, corresponding to a reduction, occurs at $E_{p,c} \simeq -0.9$ V vs. Ag/AgCl. Interestingly, these processes occur at potentials that are very similar to those found for the $[OsCl_6]^{-/2-}$ and $[OsCl_6]^{2-/3-}$ couples.[11] CV measurements on $(n$-$Bu_4N)_2Os_2Br_8$ (Figure 1) reveal redox characteristics similar to those of its chloride analogues except that the oxidation process at ~+1.1 V is clearly irreversible ($i_{p,c}/i_{p,a} << 1$).

Far-IR spectroscopy on the $[Os_2Cl_8]^{2-}$ salts recorded as Nujol mulls show small differences in ν(Os–Cl), which was located at 345 ± 5 cm^{-1}. There was no significant difference between ν(Os–Cl) of the brown crystalline form of $(PPN)_2Os_2Cl_8$ (343 cm^{-1}), which has an eclipsed rotational geometry (vide infra), and the related vibrational mode for the salt $(n$-$Bu_4N)_2Os_2Cl_8$ (347 cm^{-1}), in which the anion is essentially fully staggered.[1] The corresponding ν(Os–Br) vibration in the IR spectrum of $(n$-$Bu_4N)_2Os_2Br_8$ was found at 247 cm^{-1}. These ν(Os–X) vibrations occur at higher energies than in the spectra of corresponding $[Re_2X_8]^{2-}$ (X = Cl, Br) anions[12] due, presumably, to osmium(III) having a higher effective nuclear charge than rhenium(III). Attempts to locate the ν(Os–Os) mode in the Raman spectra of $(n$-$Bu_4N)_2Os_2X_8$ have so far been thwarted by the decomposition

(7) Evans, D. F. *J. Chem. Soc.* **1959**, 2003.
(8) Zietlow, T. C.; Klendworth, D. D.; Nimry, T.; Salmon, D. J.; Walton, R. A. *Inorg. Chem.* **1981**, *20*, 947. Under our experimental conditions the ferrocenium–ferrocene couple is at $E_{1/2}$ = +0.47 V vs. Ag/AgCl.
(9) Samples of $(Ph_4As)_2Os_2Cl_8$ slowly changed color from brown-pink to green in the solid state at room temperature over the course of several months. This transformation is currently under investigation.
(10) Geary, W. J. *Coord. Chem. Rev.* **1971**, *7*, 81.
(11) Magnuson, R. H. *Inorg. Chem.* **1984**, *23*, 387.
(12) Bratton, W. K.; Cotton, F. A.; Debeau, M.; Walton, R. A. *J. Coord. Chem.* **1971**, *1*, 121.

Table II. Atomic Positional Parameters and Equivalent Isotropic Displacement Parameters (Å^2) for Non-Hydrogen Atoms and Their Estimated Standard Deviations for $(PPN)_2Os_2Cl_8$, Green Form (**1**)[a]

atom	x	y	z	B	atom	x	y	z	B
Os(1)	0.29737 (3)	−0.07644 (5)	−0.00181 (3)	1.31 (1)	C(2132)	1.0434 (6)	0.512 (1)	0.2175 (6)	3.1 (3)*
Os(2)	0.20497 (3)	−0.03127 (5)	−0.00474 (3)	1.46 (1)	C(1113)	0.3212 (6)	0.493 (1)	−0.0353 (6)	2.9 (3)*
Os(3)	0.24246 (8)	−0.1177 (1)	−0.03219 (9)	2.53 (4)	C(1114)	0.2978 (6)	0.399 (1)	−0.0323 (6)	2.8 (3)*
Os(4)	0.27473 (7)	0.0007 (1)	0.03530 (8)	2.03 (4)	C(1115)	0.3239 (5)	0.3325 (9)	0.0162 (6)	2.4 (2)*
Cl(11)	0.3526 (1)	−0.0678 (2)	0.1029 (1)	2.62 (7)	C(1116)	0.3729 (5)	0.3639 (9)	0.0642 (6)	2.4 (2)*
Cl(12)	0.2993 (2)	−0.2474 (3)	0.0107 (2)	2.19 (9)	C(1121)	0.4860 (5)	0.6167 (8)	0.1064 (5)	1.5 (2)*
Cl(13)	0.3430 (1)	0.0742 (2)	−0.0106 (2)	3.08 (8)	C(1122)	0.4634 (5)	0.7110 (9)	0.1120 (3)	2.0 (2)*
Cl(14)	0.2880 (2)	−0.1092 (3)	−0.1025 (2)	2.5 (1)	C(1123)	0.4884 (5)	0.7962 (9)	0.0943 (6)	2.2 (2)*
Cl(21)	0.2093 (1)	0.1377 (2)	0.0027 (2)	2.59 (7)	C(1124)	0.5356 (5)	0.7854 (9)	0.0700 (6)	2.3 (2)*
Cl(22)	0.1556 (2)	−0.0062 (3)	−0.1074 (2)	3.4 (1)	C(1125)	0.5588 (5)	0.688 (1)	0.0631 (6)	2.5 (3)*
Cl(23)	0.2104 (2)	−0.0308 (3)	0.0981 (2)	3.19 (8)	C(1126)	0.5342 (5)	0.6056 (9)	0.0815 (5)	2.0 (2)*
Cl(24)	0.1542 (2)	−0.1794 (3)	−0.0174 (2)	2.9 (1)	C(1131)	0.5127 (5)	0.4163 (9)	0.1520 (5)	1.8 (2)*
Cl(31)	0.2536 (8)	−0.258 (1)	0.0250 (7)	5.6 (4)	C(1132)	0.5281 (5)	0.3619 (9)	0.1068 (6)	2.3 (2)*
Cl(32)	0.1415 (6)	−0.126 (1)	−0.0476 (7)	4.9 (4)	C(1133)	0.5822 (6)	0.300 (1)	0.1251 (6)	2.9 (3)*
Cl(33)	0.222 (1)	−0.039 (1)	−0.1217 (7)	11.3 (6)	C(1134)	0.6167 (6)	0.298 (1)	0.1854 (6)	2.8 (3)*
Cl(34)	0.3255 (7)	−0.170 (1)	−0.056 (1)	16.4 (5)	C(1135)	0.6005 (6)	0.353 (1)	0.2309 (6)	3.0 (3)*
P(11)	0.4527 (1)	0.5075 (2)	0.1297 (1)	1.58 (6)	C(1136)	0.5488 (6)	0.413 (1)	0.2136 (6)	2.9 (3)*
P(12)	0.3868 (1)	0.5083 (2)	0.2238 (1)	1.47 (6)	C(1211)	0.3663 (5)	0.3786 (9)	0.2175 (5)	1.9 (2)*
P(21)	0.9600 (2)	0.6198 (2)	0.1287 (1)	2.25 (7)	C(1212)	0.4097 (5)	0.3085 (9)	0.2482 (6)	2.3 (2)*
P(22)	0.8868 (1)	0.6049 (2)	0.2146 (1)	1.94 (7)	C(1213)	0.3987 (6)	0.206 (1)	0.2375 (6)	3.1 (3)*
N(1)	0.4258 (4)	0.5409 (7)	0.1832 (4)	1.5 (2)	C(1214)	0.3447 (6)	0.176 (1)	0.1955 (7)	3.9 (3)*
N(2)	0.9300 (4)	0.6496 (7)	0.1799 (4)	2.2 (2)	C(1215)	0.2997 (6)	0.247 (1)	0.1648 (6)	3.5 (3)*
C(1111)	0.3961 (5)	0.4626 (9)	0.0636 (5)	1.9 (2)*	C(1216)	0.3110 (6)	0.347 (1)	0.1760 (6)	2.6 (3)*
C(1112)	0.3697 (5)	0.5269 (9)	0.0136 (6)	2.2 (2)*	C(1221)	0.4298 (5)	0.5343 (9)	0.3020 (5)	1.9 (2)*
C(1223)	0.5216 (5)	0.6010 (9)	0.3728 (6)	2.5 (3)*	C(1222)	0.4864 (5)	0.5797 (9)	0.3131 (6)	2.3 (2)*
C(1224)	0.5003 (6)	0.581 (1)	0.4205 (6)	2.9 (3)*	C(2133)	1.0922 (6)	0.443 (1)	0.2385 (7)	3.5 (3)*
C(1225)	0.4417 (6)	0.539 (1)	0.4102 (6)	2.8 (3)*	C(2134)	1.1178 (7)	0.398 (1)	0.1972 (7)	3.9 (3)*
C(1226)	0.4064 (6)	0.515 (1)	0.3506 (6)	2.5 (3)*	C(2135)	1.0960 (7)	0.421 (1)	0.1351 (7)	4.0 (3)*
C(1231)	0.3179 (5)	0.5773 (9)	0.2074 (5)	1.9 (2)*	C(2136)	1.0465 (7)	0.486 (1)	0.1130 (7)	3.8 (3)*
C(1232)	0.2729 (6)	0.558 (1)	0.2363 (6)	2.8 (3)*	C(2211)	0.8751 (5)	0.4730 (9)	0.2061 (5)	1.7 (2)*
C(1233)	0.2242 (6)	0.618 (1)	0.2267 (6)	3.3 (3)*	C(2212)	0.8342 (5)	0.4376 (9)	0.1514 (6)	2.4 (3)*
C(1234)	0.2157 (6)	0.701 (1)	0.1867 (7)	3.9 (3)*	C(2213)	0.8276 (5)	0.3347 (9)	0.1421 (6)	2.4 (3)*
C(1235)	0.2584 (7)	0.721 (1)	0.1550 (7)	3.9 (3)*	C(2214)	0.8616 (6)	0.268 (1)	0.1857 (6)	2.6 (3)*
C(1236)	0.3107 (6)	0.658 (1)	0.1647 (6)	2.7 (3)*	C(2215)	0.9031 (6)	0.304 (1)	0.2391 (6)	2.7 (3)*
C(2111)	0.9907 (6)	0.734 (1)	0.1081 (6)	2.8 (3)*	C(2216)	0.9100 (5)	0.4064 (9)	0.2497 (5)	2.2 (2)*
C(2112)	1.0480 (6)	0.732 (1)	0.0974 (6)	3.5 (3)*	C(2221)	0.9174 (5)	0.6346 (9)	0.2946 (5)	1.8 (2)*
C(2113)	1.0705 (7)	0.821 (1)	0.0797 (8)	4.8 (4)*	C(2222)	0.8830 (5)	0.6222 (9)	0.3354 (5)	2.0 (2)*
C(2114)	1.0346 (8)	0.905 (1)	0.0758 (8)	5.4 (4)*	C(2223)	0.9049 (6)	0.652 (1)	0.3954 (6)	3.0 (3)*
C(2115)	0.9813 (7)	0.910 (1)	0.0848 (7)	3.8 (3)*	C(2221)	0.9645 (6)	0.693 (1)	0.4178 (6)	3.0 (3)*
C(2116)	0.9587 (6)	0.822 (1)	0.1021 (6)	2.9 (3)*	C(2225)	0.9980 (6)	0.704 (1)	0.3778 (6)	2.8 (3)*
C(2121)	0.9072 (6)	0.570 (1)	0.0602 (6)	2.8 (3)*	C(2226)	0.9754 (6)	0.679 (1)	0.3166 (6)	2.6 (3)*
C(2122)	0.8659 (5)	0.6368 (9)	0.0224 (6)	2.2 (2)*	C(2231)	0.8134 (5)	0.6622 (9)	0.1899 (6)	2.3 (2)*
C(2123)	0.8209 (6)	0.600 (1)	−0.0285 (6)	3.3 (3)*	C(2232)	0.8080 (6)	0.756 (1)	0.1620 (7)	3.7 (3)*
C(2124)	0.8152 (7)	0.500 (1)	−0.0398 (7)	4.0 (3)*	C(2233)	0.7501 (7)	0.806 (1)	0.1479 (7)	4.0 (3)*
C(2125)	0.8562 (7)	0.432 (1)	−0.0034 (8)	4.6 (4)*	C(2234)	0.7021 (7)	0.761 (1)	0.1574 (7)	4.0 (3)*
C(2126)	0.9029 (7)	0.466 (1)	0.0481 (7)	4.2 (3)*	C(2235)	0.7068 (6)	0.665 (1)	0.1831 (7)	3.8 (3)*
C(2131)	1.0200 (6)	0.531 (1)	0.1542 (6)	2.6 (3)*	C(2236)	0.7626 (6)	0.613 (1)	0.1990 (6)	2.7 (3)*

[a] Anisotropically refined atoms are given in the form of the isotropic equivalent thermal parameter defined as $^4/_3[a^2B_{11} + b^2B_{22} + c^2B_{33} + ab(\cos\gamma)B_{12} + ac(\cos\beta)B_{13} + bc(\cos\alpha)B_{23}]$. Starred values are for atoms refined isotropically.

of the complexes both in the solid state and in dichloromethane solutions.

Magnetic susceptibility measurements by the Evans and Faraday methods reveal that these salts are essentially diamagnetic.[13] Their ^{1}H NMR spectra (recorded in CD_2Cl_2 or $(CD_3)_2CO$) show only resonances due to the cations that are not significantly different from the ^{1}H NMR spectra of the simple chloride salts of the cations. Such non-contact-shifted resonances are also in accord with the observed diamagnetism of the complexes. These observations support the diamagnetic triply bonded configuration $\sigma^2\pi^4\delta^2\delta^{*2}$ as being the principal contributor to the ground state, a conclusion that is supported by SCF–Xα–SW calculations[1] and the previous interpretation of the electronic absorption spectra of the $[Os_2Cl_8]^{2-}$ anion.[14]

Structure Determination on Crystals of $(PPN)_2Os_2Cl_8$. In our previous preliminary report,[5] we described the results of an X-ray structure analysis on crystals of $(PPN)_2Os_2Cl_8$ (green form, **1**) as determined at 22 °C. The structure of this complex was similar to that of other $[M_2X_8]^{n-}$ anions in two ways; namely, two $OsCl_4$ units are joined together by a remarkably short osmium–osmium bond (2.195 Å) and a disorder of the Os–Os unit in the nearly cubic array of chlorine atoms was observed (in this case with 64% occupancy for the major orientation). However, one important structural difference was observed for the $[Os_2Cl_8]^{2-}$ anion; the two $OsCl_4$ units were found to be rotated relative to one another by a twist (torsional) angle χ of 13.9 (4.5)° for the major orientation (χ = 10.3 (6.2)° for the minor orientation) while the eclipsed conformation (χ = 0°) is found in salts of $[Mo_2X_8]^{4-}$ (X

(13) The complexes $(PPN)_2Os_2Cl_8$ and $(n\text{-}Bu_4N)_2Os_2Br_8$ were found to be diamagnetic as determined by the Evans method (CH_2Cl_2, 22 °C). This is also the case for $(n\text{-}Bu_4N)_2Os_2Cl_8$ ($\chi_g = -0.47 \times 10^{-6}$ cgsu), although after allowance had been made for diamagnetic corrections there appears to be a small residual paramagnetism ($\chi_m' \simeq 100 \times 10^{-6}$ cgsu). Measurements on solid samples of these two salts with a Cahn/Ventron Faraday magnetic susceptibility balance (23 °C) gave χ_g values of −0.35 $\times 10^{-6}$ and −0.36 $\times 10^{-6}$ cgsu, respectively. When allowance is made for diamagnetic corrections, we get $\chi_m' = 313 \times 10^{-6}$ and 250×10^{-6} cgsu, respectively. Related measurements on a sample of $(n\text{-}Bu_4N)_2Os_2Br_8$ gave $\chi_g = -0.16 \times 10^{-6}$ and $\chi_m' = 514 \times 10^{-6}$ cgsu. We thank Professor T. J. Smith (Kalamazoo College) for these Faraday balance measurements.

(14) Spectra were recorded on CH_2Cl_2 solutions in the region 1800–250 nm. Data for the chloride complexes are reported in ref 1 and 5. Data for $(n\text{-}Bu_4N)_2Os_2Br_8$ is as follows (λ_{max} in nm, ϵ_{max} values given in parentheses): ~950 sh, 695 (258), 500 sh, 430 sh, 340 (13 000), 300 (12 200).

Table III. Atomic Positional Parameters and Equivalent Isotropic Displacement Parameters (Å^2) for Non-Hydrogen Atoms and Their Estimated Standard Deviations for $(PPN)_2Os_2Cl_8$, Brown Form (**2**)[a]

atom	*x*	*y*	*z*	*B*
Os(1)	0.48156 (1)	0.03437 (3)	0.52121 (2)	2.440 (9)
Os(3)	0.45644 (3)	−0.00462 (7)	0.42949 (4)	2.81 (2)
Cl(1)	0.54577 (7)	0.1601 (2)	0.6160 (1)	4.59 (5)
Cl(2)	0.47428 (7)	0.0488 (2)	0.35025 (9)	4.33 (5)
Cl(3)	0.39883 (6)	−0.0600 (2)	0.4461 (1)	4.80 (5)
Cl(4)	0.41717 (6)	0.1503 (2)	0.4118 (1)	4.87 (6)
P(1)	0.33660 (5)	0.4269 (1)	0.60405 (8)	2.49 (4)
P(2)	0.39167 (5)	0.6036 (1)	0.72187 (8)	2.48 (4)
N	0.3812 (2)	0.5127 (4)	0.6672 (3)	3.1 (1)
C(111)	0.2868 (2)	0.4600 (5)	0.4879 (3)	2.6 (1)*
C(112)	0.2475 (2)	0.3899 (6)	0.4191 (3)	3.6 (1)*
C(113)	0.2090 (2)	0.4177 (6)	0.3297 (4)	4.3 (2)*
C(114)	0.2094 (3)	0.5119 (7)	0.3065 (4)	4.6 (2)*
C(115)	0.2499 (2)	0.5794 (6)	0.3746 (4)	4.3 (2)*
C(116)	0.2879 (2)	0.5538 (6)	0.4649 (4)	3.5 (1)*
C(121)	0.2967 (2)	0.3911 (5)	0.6278 (3)	2.7 (1)*
C(122)	0.2354 (2)	0.3987 (6	0.5606 (3)	3.5 (1)*
C(123)	0.2068 (2)	0.3786 (6)	0.5848 (4)	4.4 (2)*
C(124)	0.2371 (3)	0.3526 (7)	0.6703 (4)	5.0 (2)*
C(125)	0.2985 (3)	0.3439 (7)	0.7373 (4)	4.8 (2)*
C(126)	0.3280 (2)	0.3645 (6)	0.7140 (3)	3.7 (1)*
C(131)	0.3763 (2)	0.3227 (5)	0.6194 (3)	2.8 (1)*
C(132)	0.3809 (2)	0.2353 (6)	0.6565 (4)	3.6 (1)*
C(133)	0.4126 (2)	0.1579 (6)	0.6667 (4)	4.4 (2)*
C(134)	0.4396 (3)	0.1694 (6)	0.6397 (4)	4.6 (2)*
C(135)	0.4358 (3)	0.2562 (7)	0.6052 (5)	5.6 (2)*
C(136)	0.4027 (3)	0.3340 (7)	0.5925 (4)	4.6 (2)*
C(211)	0.4613 (2)	0.5905 (5)	0.8372 (3)	2.6 (1)*
C(212)	0.4852 (2)	0.4971 (6)	0.8700 (3)	3.5 (1)*
C(213)	0.5372 (3)	0.4841 (6)	0.9612 (4)	4.3 (2)*
C(214)	0.5654 (3)	0.5674 (6)	1.0175 (4)	4.4 (2)*
C(215)	0.5419 (3)	0.6583 (6)	0.9843 (4)	4.4 (2)*
C(216)	0.4891 (2)	0.6714 (6)	0.8932 (3)	3.5 (1)*
C(221)	0.3927 (2)	0.7149 (5)	0.6784 (3)	2.8 (1)*
C(222)	0.3671 (2)	0.7986 (6)	0.6712 (3)	3.4 (1)*
C(223)	0.3671 (2)	0.8834 (6)	0.6350 (4)	3.9 (2)*
C(224)	0.3951 (3)	0.8836 (6)	0.6107 (4)	4.5 (2)*
C(225)	0.4215 (3)	0.7993 (6)	0.6189 (4)	4.6 (2)*
C(226)	0.4198 (2)	0.7130 (6)	0.6512 (4)	3.8 (2)*
C(231)	0.3375 (2)	0.6194 (5)	0.7206 (3)	2.6 (1)*
C(232)	0.3539 (2)	0.6213 (6)	0.8015 (4)	3.8 (2)*
C(233)	0.3097 (3)	0.6313 (7)	0.7963 (4)	4.6 (2)*
C(234)	0.2530 (2)	0.6401 (6)	0.7157 (4)	4.3 (2)*
C(235)	0.2363 (2)	0.6405 (6)	0.6359 (4)	4.2 (2)*
C(236)	0.2802 (2)	0.6308 (6)	0.6392 (3)	3.5 (1)*

[a] See footnote *a* of Table II.

= Cl, Br), $[W_2Cl_8]^{4-}$, $[Tc_2Cl_8]^{3-}$, and $[Re_2X_8]^{2-}$ (X = Cl, Br).[2-4,15] The fact that the $[Os_2Cl_8]^{2-}$ anion has a nonzero torsional angle was explained[5] as follows; since the complex is essentially diamagnetic, the ground-state configuration describing the osmium–osmium bonding is the diamagnetic triply bonded $\sigma^2\pi^4\delta^2\delta^{*2}$ configuration. Since there is no net δ component to the Os–Os bonding, free rotation of the $OsCl_4$ units about the osmium–osmium bond can occur.[2] This is in contrast to the case for the Mo, W, Tc, and Re species cited above, which have a net δ-bonding component in which overlap of the δ bond is maximized for an eclipsed structure ($\chi = 0°$). However, the structure solution and its attendent interpretation were plagued by two problems: (1) the crystal used was of rather poor quality, and (2) the thermal ellipsoids of one set of four chlorine atoms about one of the osmium centers (Os(3) of the minor orientation) were rather large. We suspected that the latter effect was caused by either excess thermal vibration of this set of chlorine atoms or that the chlorine atoms bound to Os(3) in the minor orientation were at slightly different locations than those associated with the major orientation. In order to resolve this problem, we have carried out a structure determination on the green form **1** of $(PPN)_2Os_2Cl_8$ at low temperature (−190 °C).

Table IV. Selected Distances, Angles, and Torsion Angles and Their Estimated Standard Deviations for $(PPN)_2Os_2Cl_8$, Green Form (**1**)[a]

major orientation		minor orientation		major orientation		minor orientation	
			Distances (Å)				
Os(1)–Os(2)	2.206 (1)	Os(3)–Os(4)	2.18 (2)	Os(2)–Cl(21)	2.274 (2)	Os(4)–Cl(11)	2.19 (3)
Os(1)–Cl(11)	2.347 (1)	Os(3)–Cl(31)	2.26 (1)	Os(2)–Cl(22)	2.301 (3)	Os(4)–Cl(13)	2.36 (2)
Os(1)–Cl(12)	2.311 (1)	Os(3)–Cl(32)	2.26 (2)	Os(2)–Cl(23)	2.318 (2)	Os(4)–Cl(21)	2.35 (3)
Os(1)–Cl(13)	2.319 (2)	Os(3)–Cl(33)	2.23 (2)	Os(2)–Cl(24)	2.282 (4)	Os(4)–Cl(23)	2.40 (2)
Os(1)–Cl(14)	2.289 (3)	Os(3)–Cl(34)	2.26 (3)	Os–Cl (av)	2.313 [9]	Os–Cl (av)	2.29 [3]
			Angles (deg)				
Os(2)–Os(1)–Cl(11)	103.79 (4)	Os(4)–Os(3)–Cl(31)	104 (1)	Cl(11)–Os(1)–Cl(14)	152.94 (9)	Cl(31)–Os(3)–Cl(34)	85.8 (8)
Os(2)–Os(1)–Cl(12)	105.00 (4)	Os(4)–Os(3)–Cl(32)	106 (1)	Cl(12)–Os(1)–Cl(13)	152.17 (7)	Cl(32)–Os(3)–Cl(33)	88.0 (8)
Os(2)–Os(1)–Cl(13)	102.80 (6)	Os(4)–Os(3)–Cl(33)	103 (2)	Cl(12)–Os(1)–Cl(14)	85.74 (8)	Cl(32)–Os(3)–Cl(34)	149.7 (7)
Os(2)–Os(1)–Cl(14)	103.27 (9)	Os(4)–Os(3)–Cl(34)	105.2 (9)	Cl(13)–Os(1)–Cl(14)	89.2 (2)	Cl(33)–Os(3)–Cl(34)	83.0 (8)
Os(1)–Os(2)–Cl(21)	104.54 (7)	Os(3)–Os(4)–Cl(11)	103 (1)	Cl(21)–Os(2)–Cl(22)	85.8 (1)	Cl(11)–Os(4)–Cl(13)	88.4 (5)
Os(1)–Os(2)–Cl(22)	104.28 (9)	Os(3)–Os(4)–Cl(13)	97 (1)	Cl(21)–Os(2)–Cl(23)	86.2 (1)	Cl(11)–Os(4)–Cl(21)	149.9 (7)
Os(1)–Os(2)–Cl(23)	102.66 (6)	Os(3)–Os(4)–Cl(21)	107 (1)	Cl(21)–Os(2)–Cl(24)	152.6 (1)	Cl(11)–Os(4)–Cl(23)	92 (1)
Os(1)–Os(2)–Cl(24)	102.8 (1)	Os(3)–Os(4)–Cl(23)	98.8 (7)	Cl(22)–Os(2)–Cl(23)	153.0 (2)	Cl(13)–Os(4)–Cl(21)	89 (2)
Os–Os–Cl (av)	103.75 [35]	Os–Os–Cl (av)	102.8 [13]	Cl(22)–Os(2)–Cl(24)	85.8 (1)	Cl(13)–Os(4)–Cl(23)	163.8 (7)
Cl(11)–Os(1)–Cl(12)	86.49 (5)	Cl(31)–Os(3)–Cl(32)	88.9 (5)	Cl(23)–Os(2)–Cl(24)	89.8 (1)	Cl(21)–Os(4)–Cl(23)	82.5 (5)
Cl(11)–Os(1)–Cl(13)	85.68 (7)	Cl(31)–Os(3)–Cl(33)	152.0 (8)				
			Torsion Angles (deg)				
Cl(11)–Os(1)–Os(2)–Cl(23)	10.58 (11)	Cl(31)–Os(3)–Os(4)–Cl(11)	38.76 (35)	Cl(14)–Os(1)–Os(2)–Cl(22)	12.77 (13)	Cl(34)–Os(3)–Os(4)–Cl(13)	39.13 (53)
Cl(12)–Os(1)–Os(2)–Cl(24)	13.30 (12)	Cl(32)–Os(3)–Os(4)–Cl(23)	37.52 (38)	Cl–Os–Os–Cl (av)	11.45 [85]	Cl–Os–Os–Cl (av)	39.8 [14]
Cl(13)–Os(1)–Os(2)–Cl(21)	9.86 (9)	Cl(33)–Os(3)–Os(4)–Cl(21)	44.18 (45)				

[a] Numbers in parentheses are estimated standard deviations in the least significant digits. Numbers in brackets are the weighted deviations.

(15) Huang, H. W.; Martin, D. S. *Inorg. Chem.* **1985**, *24*, 96.

Table V. Selected Distances and Angles and Their Estimated Standard Deviations for $(PPN)_2Os_2Cl_8$, Brown Form (**2**)[a]

major orientation		minor orientation	
	Distances (Å)		
Os(1)–Os(1)	2.212 (1)	Os(3)–Os(3)	2.211 (1)
Os(1)–Cl(1)	2.318 (2)	Os(3)–Cl(1)	2.324 (2)
Os(1)–Cl(2)	2.290 (2)	Os(3)–Cl(2)	2.305 (2)
Os(1)–Cl(3)	2.328 (2)	Os(3)–Cl(3)	2.327 (2)
Os(1)–Cl(4)	2.313 (2)	Os(3)–Cl(4)	2.375 (2)
Os–Cl (av)	2.312 [8]	Os–Cl (av)	2.333 [16]
	Angles (deg)		
Os(1′)–Os(1)–Cl(1)	104.26 (5)	Os(3′)–Os(3)–Cl(1)	103.98 (6)
Os(1′)–Os(1)–Cl(2)	103.34 (5)	Os(3′)–Os(3)–Cl(2)	102.43 (6)
Os(1′)–Os(1)–Cl(3)	102.17 (5)	Os(3′)–Os(3)–Cl(3)	102.30 (6)
Os(1′)–Os(1)–Cl(4)	104.61 (5)	Os(3′)–Os(3)–Cl(4)	100.97 (7)
Os–Os–Cl (av)	103.60 [55]	Os–Os–Cl (av)	102.47 [61]
Cl(1)–Os(1)–Cl(2)	86.00 (6)	Cl(1)–Os(3)–Cl(2)	85.51 (6)
Cl(1)–Os(1)–Cl(3)	153.57 (6)	Cl(1)–Os(3)–Cl(3)	89.49 (7)
Cl(1)–Os(1)–Cl(4)	88.27 (7)	Cl(1)–Os(3)–Cl(4)	155.02 (7)
Cl(2)–Os(1)–Cl(3)	87.82 (6)	Cl(2)–Os(3)–Cl(3)	155.25 (7)
Cl(2)–Os(1)–Cl(4)	152.02 (6)	Cl(2)–Os(3)–Cl(4)	90.48 (6)
Cl(3)–Os(1)–Cl(4)	85.25 (6)	Cl(3)–Os(3)–Cl(4)	83.90 (7)

[a] See footnote *a* of Table IV.

Table VI. Electrochemical Properties of Salts of the $[Os_2X_8]^{2-}$ Anions (X = Cl, Br)

complex	voltammetric potentials[a]	
	$E_{1/2}$[b]	$E_{p,c}$
$(PPN)_2Os_2Cl_8$	1.19 (100)	−0.85
$(n\text{-}Bu_4N)_2Os_2Cl_8$	1.16 (115)	−0.90
$(Ph_4As)_2Os_2Cl_8$	1.16 (100)	−0.90
$(n\text{-}Bu_4N)_2Os_2Br_8$	1.14[c]	−0.75

[a] In volts vs. Ag/AgCl with a Pt-bead electrode and 0.1 M tetra-*n*-butylammonium hexafluorophosphate (TBAH) as supporting electrolyte in dichloromethane. [b] Values of $E_{p,a} - E_{p,c}$ (in mV) at a sweep rate of 200 mV/s are given in parentheses. [c] $E_{p,a}$ value.

The pertinent structural data for **1** are listed in Tables I, II, and IV, and an ORTEP view of the anion in this salt is shown in Figure 2. In a manner similar to that observed for salts of other $[M_2X_8]^{n-}$ anions, a disorder is present in which the Os–Os unit is randomly present in two orientations with the major orientation having a 71% occupancy. The osmium–osmium distances associated with the major and minor orientations are 2.206 (1) and 2.18 (2) Å, respectively. Such a difference in metal–metal bond lengths has been previously encountered in the structures of other $[M_2X_8]^{n-}$ species when this type of disorder is present.[2] What is especially remarkable and unexpected is that a set of chlorine atoms (Cl(31), Cl(32), Cl(33), and Cl(34)) associated with the minor orientation (Os(3)) are indeed found at different locations than the chlorine atoms of the major orientation.[16] This gives rise to the existence of two different rotamers in the solid-state structure of the green form of $(PPN)_2Os_2Cl_8$. The major orientation has a twist angle of 11.45 [85]° while the minor orientation has a much larger twist angle of 39.8 [14]°. It had not previously been anticipated that this type of disorder would be preserved when the close to cubic array of chlorine atoms had become distorted toward a square-antiprismatic arrangement. The structure of **1** represents the first example of its kind in multiple-bond chemistry.

(16) It should be noted that the chlorine set Cl(12), Cl(14), Cl(22), and Cl(24) associated with the major orientation makes reasonable bond distances and angles with Os(3). Thus, the possibility that the chlorines are completely disordered about Os(3) cannot be entirely ruled out. However, the model we used sets the mul iplicity of those chlorines on Os(1) and Os(2) that are not also connected to Os(4) equal to the multiplicity of Os(1) and Os(2). The agreement in the temperature factors between the fully occupied set of chlorines (B_{av} = 2.8 [3] Å^2 for Cl(12), Cl(14), Cl(22), and Cl(24)) and this partially occupied set (B_{av} = 2.7 [5] Å^2 for Cl(11), Cl(13), Cl(21), and Cl(23)) supports this assumption. The large B_{av} value for the third set of chlorines (i.e. those bound to Os(3)) is a result of the large anisotropy of the thermal ellipsoids.

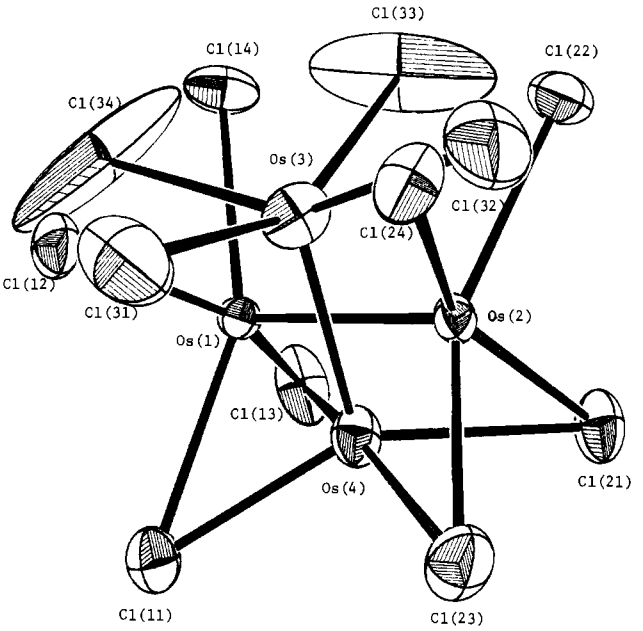

Figure 2. ORTEP view of the $[Os_2Cl_8]^{2-}$ anion in **1** at −190 °C. The thermal ellipsoids are drawn at the 50% probability level. There are two disordered orientations of the osmium–osmium unit. Os(1) and Os(2) were refined to an occupancy of 71.4% with an Os(1)–Os(2) distance of 2.206 (1) Å. The Os(3)–Os(4) vector is approximately perpendicular to this with a bond distance of 2.18 (2) Å.

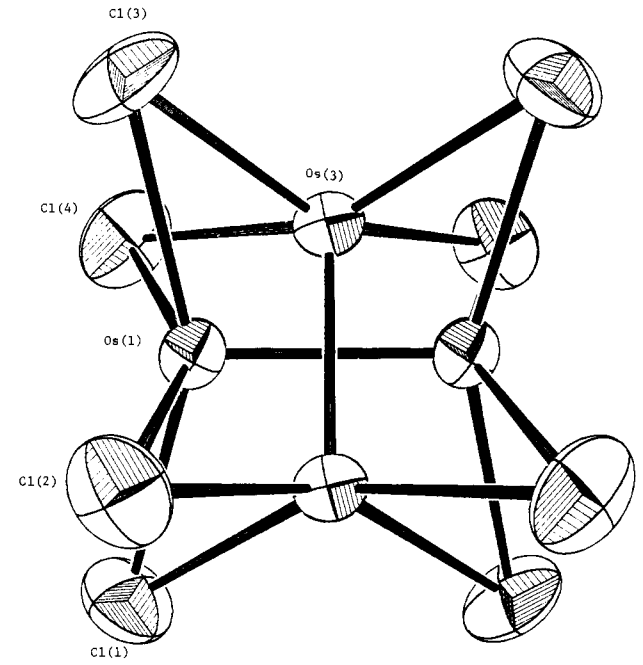

Figure 3. ORTEP view of the $[Os_2Cl_8]^{2-}$ anion in **2** at 22 °C. Thermal ellipsoids are drawn at the 50% probability level. There are two disordered orientations of the osmium–osmium unit. Os(1) was refined to an occupancy of 69.5% with an Os(1)–Os(1′) distance of 2.212 (1) Å. The Os(3)–Os(3′) vector is perpendicular to this with a bond distance of 2.211 (1) Å.

The brown crystalline form **2** of $(PPN)_2Os_2Cl_8$ also provided crystals that were suitable for an X-ray structure analysis. The atomic positional parameters are listed in Table III, a selection of important bond distances and angles are given in Table V, and an ORTEP representation of the $[Os_2Cl_8]^{2-}$ anion in this room-temperature structure determination is presented in Figure 3. As is apparent from the ORTEP drawing, **2** has the same type of disorder as is observed in **1** with the major orientation having a 70% occupancy. The osmium–osmium bond lengths for the two orientations are the same, viz., 2.212 (1) Å for Os(1)–Os(1′) and 2.211 (1) Å for Os(3)–Os(3′). The twist angle for both orien-

Table VII. Selected Structural Parameters for Salts of the $[Os_2Cl_8]^{2-}$ Anion

complex	Os–Os, Å	Os–Cl, Å	Os–Os–Cl, deg	twist angle, deg
$(n\text{-}Bu_4N)_2Os_2Cl_8$[a]	2.182 (1)	2.322 [6]	104.2 (3)	49.0 [3]
$(PPN)_2Os_2Cl_8$ (**1**)				
major	2.206 (1)	2.313 [9]	103.7 [4]	11.4 [8]
minor	2.18 (2)	2.29 [3]	102.8 [13]	39.8 [14]
$(PPN)_2Os_2Cl_8$ (**2**)				
major	2.212 (1)	2.312 [8]	103.6 [6]	0.0
minor	2.211 (1)	2.333 [16]	102.5 [6]	0.0

[a] Data taken from ref 1.

tations is required by the crystallographic symmetry present to be 0.0°.

The structural parameters of the PPN cations in **1** and **2** are essentially identical, with d(P–N) = 1.575 [12] and 1.577 [6] Å and the P–N–P angle being 142.4 [5] and 142.5 [3]° in **1** and **2**, respectively.

A comparison is made in Table VII between selected structural parameters for **1** and **2** as determined in the present study and those for $(n\text{-}Bu_4N)_2Os_2Cl_8$ (from ref 1). The structure of the bromide analogue $(n\text{-}Bu_4N)_2Os_2Br_8$ is very similar to that of its chloride analogue.[1] In the tetra-*n*-butylammonium salt, the $[Os_2Cl_8]^{2-}$ anion possesses an essentially completely staggered rotational geometry (χ = 49°) and the shortest Os–Os bond length. This probably reflects a minimization of any nonbonded Cl···Cl repulsions. However, that the latter interactions do not dictate the rotational geometry is clearly established by the present work. The green and brown crystalline forms of $(PPN)_2Os_2Cl_8$ have very similar Os–Os and Os–Cl bond lengths and Os–Os–Cl bond angles yet the twist angles are quite different (Table VII). In systems such as these where there is no electronic barrier to rotation ($\sigma^2\pi^4\delta^2\delta^{*2}$ configuration),[1,2] this difference can only be attributed to differences in crystal-packing forces, which are clearly dictating the rotational geometry.[17] This is certainly reasonable since plots of X···X van der Waals energies against internuclear distances for $[M_2X_8]^{n-}$ species indicate[20] that for X = Cl we may not yet be in a region where repulsion is important and, by implication, a staggered geometry necessarily preferred. In the case of the essentially fully staggered geometry in the salt $(n\text{-}Bu_4N)_2Os_2Cl_8$, the Cl···Cl distances average to 3.742 [16] Å, while in the eclipsed form of $(PPN)_2Os_2Cl_8$ (**2**) the distance is much shorter (3.299 [24] Å).

As mentioned earlier, the chlorine atoms bound to Os(3) in the room-temperature structure solution[5] have large thermal ellipsoids, which are thought to be caused by either excess thermal vibration or uncertainty in the locations of these chlorine atoms. Since the thermal ellipsoids of the chlorine atoms about Os(3) in **1** are still quite large even in our low-temperature structure determination, this suggests that the effect is not due to excess thermal motion but rather to uncertainty in the locations of the chlorine atoms about Os(3). Consequently, we are led to believe that **1** is the less thermodynamically stable form of $(PPN)_2Os_2Cl_8$. Note that the brown form **2** results when this complex is crystallized slowly from more dilute dichloromethane solutions of $(PPN)_2Os_2Cl_8$. The green form **1** is formed much more rapidly from concentrated dichloromethane solutions of $(PPN)_2Os_2Cl_8$. This difference is thermodynamic stability is supported by two further observations. First, the unit cell volume of **2** is slightly smaller than that of the green form at room temperature[5] (6798 vs. 6935 Å^3). This results in more efficient crystal packing for **2** and also accounts for the fact that the thermal ellipsoids of the chlorine atoms in **2** are much smaller than those of **1**. Second, when samples of **1** and **2** are heated in argon-filled capillaries, the crystal surface of **1** forms pink islands of **2** at ca. +175 °C while **2** itself is unchanged. Eventually, the crystals of **1** disintegrate and eventually decompose at 280 °C, which is also the decomposition temperature of **2**.

Concluding Remarks. The isolation of salts of the $[Os_2X_8]^{2-}$ anions (X = Cl, Br) has provided an excellent opportunity to expand the chemistry of homoleptic halide complexes of multiply bonded dimetal species to include for the first time the platinum metals. The unexpected shortness of the Os–Os bonds in these triply bonded complexes (the distances are much shorter than those encountered in any previously characterized diosmium complexes)[2,21,22] attests to the strength of these interactions, and the varied rotational geometries encountered in the green and brown crystalline forms of $(PPN)_2Os_2Cl_8$ reflect the absence of significant nonbonded Cl···Cl repulsions in dictating the rotational geometry within the anion. The $[Os_2X_8]^{2-}$ anions are very reactive toward phosphines, carbon monoxide, isocyanides, and many other ligands, and these aspects of their chemical reactivity are currently under investigation. The latter results will be reported in due course.

Acknowledgment. We thank the donors of the Petroleum Research Fund, administered by the American Chemical Society, and the National Science Foundation (Grant No. CHE85-06702) for partial support of this work.

Registry No. $Os_2(O_2CCH_3)_4Cl_2$, 81519-41-7; $Os_2(O_2C\text{-}n\text{-}C_6H_7)_4Cl_2$, 83292-95-9; $(PPN)_2Os_2Cl_8$, 97523-24-5; $(Ph_4As)_2Os_2Cl_8$, 97523-36-9; $(n\text{-}Bu_4N)_2Os_2Cl_8$, 97523-37-0; $(n\text{-}Bu_4N)_2Os_2Br_8$, 97523-38-1; Os, 7440-04-2.

Supplementary Material Available: Listings of thermal parameters (Tables S1 and S2) and complete listings of all bond distances (Tables S3 and S4) and bond angles (Tables S5 and S6) for both structures (14 pages); listings of observed and calculated structure factors for both structures (43 pages). Ordering information is given on any current masthead page.

(17) There is evidence from recent crystallographic studies on the dimolybdenum(II) iodide complexes $Mo_2I_4(\mu\text{-}Ph_2PCH_2PPh)_2$[18] and $Mo_2I_4(\mu\text{-}Ph_2PCH_2CH_2PPh_2)_2$[19] that crystal-packing forces can dictate to some extent the rotational geometry even in systems that have a quadruple bond.

(18) Fanwick, P. E.; Harwood, W. S.; Walton, R. A. *Inorg. Chim. Acta*, in press.

(19) Cotton, F. A.; Dunbar, K. R.; Matusz, M. *Inorg. Chem.* **1986**, *25*, 3641.

(20) Cotton, F. A.; Gage, L. D.; Mertis, K.; Shive, L. W.; Wilkinson, G. *J. Am. Chem. Soc.* **1976**, *98*, 6922.

(21) Chakravarty, A. R.; Cotton, F. A.; Tocher, D. A. *Inorg. Chem.* **1984**, *23*, 4693.

(22) Chakravarty, A. R.; Cotton, F. A.; Tocher, D. A. *Inorg. Chem.* **1984**, *23*, 4697.